

Synthesis of soluble polyimide derived from novel naphthalene diamines for liquid crystal alignment layers and a preliminary study on the mechanism of imidization

Cite this: DOI: 10.1039/c3ra42098a

Senlin Xia, Zhen Sun, Longfei Yi and Yinghan Wang*

Novel functional diamine, 6-hexyloxy-naphthalen-3',5'-diaminobenzoate (**N6**) containing a rigid naphthalene unit, was molecularly designed and successfully synthesized. PIs (polyimides) were obtained by copolymerization of **N6**, 3,3'-dimethyl-4,4'-methylenediamine (DMMDA) and 4,4'-oxydiphthalic anhydride (ODPA). The structures of the intermediates, diamines and PIs were confirmed by FT-IR and ¹H NMR spectra. All PIs obtained could be dissolved in polar aprotic solvents and low-boiling-point solvents. PI (polyimide) films attained using a casting method showed favorably high transmittance above 95% in the wave length range of 400–700 nm and could align LCs vertically before and after rubbing treatment. PI-**N6** derived from **N6**, DMMDA and ODPA exhibited a much higher temperature at a 5% weight loss (T_5) compared with the corresponding PI-**C6** from 4-hexyloxy-biphenyl-3',5'-diaminobenzoate (**C6**). For PI-**N6**, the weight ratio of the side chains was smaller than that of PI-**C6**, but a much higher T_5 was attained. The results demonstrated that the introduction of a naphthalene unit into the side chain could effectively improve the thermal stability of PI without sacrificing its solubility. Moreover, the outstanding thermal stability of the PIs was explained in a preliminary manner by the imidization reaction mechanism.

Received 29th April 2013,
Accepted 5th June 2013

DOI: 10.1039/c3ra42098a

www.rsc.org/advances

1. Introduction

Aromatic polyimides (PIs) are considered to be relevant materials for advanced technologies because of their outstanding thermal, mechanical, and chemical stability.^{1,2} However, it is known that fully aromatic PIs are very often insoluble in most organic solvents because of the rigidity of their backbone and strong interchain interactions, which greatly limits their application in many fields such as microelectronics and liquid crystal displays (LCD).³ The increasing demands of this application have stimulated extensive research on soluble PIs that can exhibit certain advantageous properties. Typical approaches include the introduction of flexible or kinked linkages,^{4,5} bulky substituents,^{6–8} noncoplanar structures,^{9,10} and spiro-skeletons^{11,12} into the polymer backbone.

For PI materials used as alignment layers in the field of LCD devices, high transparency is also required in addition to easy processability. To improve the optical transparency of PIs, methods such as the introduction of the fluorinated groups and a twisted structure, and the replacement of aromatic

groups with alicyclic groups to form the so-called alicyclic PIs are by far the most effective approaches.^{13–16}

To attain good quality LCD devices, many factors should be taken into account such as the viewing angle, optical contrast, response time, and LC alignment ability in addition to the solubility and optical transparency. However, the pretilt angle plays the most important role in determining the optical and electrical performance of industrial LCD devices. The conventional main-chain-type PI alignment layer can achieve only a small pretilt angle.^{17,18} PIs that induce a high pretilt angle are needed for specially tailored display applications. For example, a vertical alignment method has been used to improve the alignment of the LCs with negative dielectric anisotropy for a faster response time and a higher contrast ratio compared with those of twisted nematic LCDs.¹⁹ Some recent reports have pointed out that alkyl side chains greatly elevate the pretilt angle and that alkyl side-chain PIs could be very promising candidates for excellent LC alignment layers.^{17,20–24} As widely reported, the long alkyl side chain with more than 6 carbon atoms is well known for its positive effect on the LC alignment and the attainment of a high pretilt angle.²⁵ Those materials that induce a high pretilt angle often contain side chains composed of rigid units and alkyl groups that tend to stick out of the surface of the PI.^{26–28} However, the existence of side chains unfortunately sacrifices the thermal stability of

College of Polymer Science and Engineering, State Key Laboratory of Polymer Materials Engineering, Sichuan University, Chengdu 610065, China.

E-mail: wang_yh@scu.edu.cn; Tel: 028-85460823

soluble PIs due to the loose chain-packing and weak interchain interactions resulting from the introduction of long side chains. One of the most significant ideas is that the thermal stability of soluble PIs can be improved by adjusting the chemical structure of side chain, while a high pretilt angle is achieved simultaneously.

Our previous work has been mainly focused on the solubility of PIs and high pretilt angles generated by the PI film without serious consideration of its lowered thermal stability.²⁶ It is well-known that materials used in LCD devices should be thermally resistant because LCD devices usually generate a great amount of heat while operating. However, to the best of our knowledge, the thermal stability of soluble PIs which can align LCs vertically has not been carefully studied. So this area of research is worth being paid enough attention to and carried out.

The objectives of this research were to synthesize organo-soluble PIs having improved thermal stability and high pretilt angles at the same time, and to preliminarily investigate the mechanism of imidization. We focused on a specially designed novel PI containing naphthalene side chains as the alignment layer having a high pretilt angle. Properties such as solubility, optical transparency, surface energy and pretilt angle were investigated. The focus has especially been on the improved thermal stability, and the results have been compared with our previous studies.²⁶ In addition, the favorable thermal stability of the PIs was preliminarily explained by the imidization reaction mechanism. The novel PIs obtained will hopefully be applied in vertical-alignment-mode LCD devices.

2. Experimental

2.1 Materials

4,4'-Oxydiphthalic anhydride (ODPA; >98%, Shanghai Research Institute of Synthetic Resins), was purified by recrystallization from acetic anhydride and dried under vacuum prior to use. 3,3'-Dimethyl-4,4'-methylenediamine (DMMDA) was purchased from Shanghai EMST Corp. (Shanghai, China) and purified by recrystallization from ethanol. Naphthalene-2,6-diol was acquired from Shanghai Jingsai chemical Corp. (Shanghai, China). 1-Bromopentane was obtained from Shanghai Reagent Co. Ltd. (Shanghai, China). 3,5-Dinitrobenzoyl chloride was attained from Taixing Re-fined Chemical Co. Ltd. (Jiangsu, China) and 5% palladium activated carbon was gained from Guoyao Corp. (Shanghai, China). Triethylamine (TEA) was obtained from Chengdu Kelong Chemical Reagent Corp. (Chengdu, China). *N*-Methyl-2-pyrrolidone (NMP) was distilled under reduced pressure after stirring over calcium hydride for 24 h and stored over 4 Å molecular sieves before use. Dimethylsulfoxide (DMSO), dimethylformamide (DMF), dimethylacetamide (DMAc), tetrahydrofuran (THF), chloroform (TCM) and *m*-cresol were used as received. Nematic LC E7 ($n_o = 1.521$, $\Delta n = 0.22$, $T_{n-1} = 60$ °C) was purchased from Shijiazhuang Crown Chem-Tech. Co. Ltd.

2.2 Measurement

Nuclear magnetic resonance (¹H NMR) spectra were obtained using a 400 MHz Unity Inova 400 spectrophotometer using CDCl₃ or DMSO as a solvent. Fourier transform infrared (FTIR) spectra were recorded with a Nicolet 560 FTIR spectrometer (Thermo Nicolet Corporation, USA). A spin-coat process was executed using a KW-4A spinner from the Institute of Microelectronics of the Chinese Academy of Sciences (Beijing, China). The pretilt angles of the LCs were measured using the crystal rotation method using a pretilt angle tester from the Changchun Institute of Optics, Fine Mechanics and Physics (Changchun, China), and at least five different points on cells were selected for measurement. The rubbing process was operated using a rubbing machine from TianLi Co. Ltd. (Chengdu, China). Thermogravimetric Analysis (TGA) was performed using a DuPont TGA2100 at a heating rate of 10 °C min⁻¹ under a nitrogen atmosphere. Differential scanning calorimetry (DSC) testing was performed on a PerkinElmer DSC7 differential scanning calorimeter at a scanning rate of 10 °C min⁻¹ under flowing nitrogen (30 cm³ min⁻¹), and the glass-transition temperatures (T_g s) were read from the DSC curves at the same time. The contact angles of deionized water and diiodomethane on the surface of PI films were measured using a Kruss DSA100 goniometer system (Kruss GmbH, Germany). Each sample was tested three times and the mean values of contact angle as well as surface free energy were calculated. The inherent viscosity of the polymer was measured at a concentration of 0.5 g dL⁻¹ in NMP using an Ubbelohde-type viscometer at 30 °C. Gel permeation chromatography of soluble polymers was performed using an Applied Bio system at 70 °C with two PL gel 5 µm mixed-C columns.

2.3 Synthesis of the monomers

2.3.1 Synthesis of 6-hexyloxy-2-hydronaphthalen (a). A mixture of 200 mL of methanol, 9.12 g (0.057 mol) of naphthalene-2,6-diol and 5.00 g (0.089 mol) of potassium hydroxide was placed into a 500 mL flask equipped with a magnetic stirrer and a condenser. The mixture was stirred until a complete dissolution was achieved and heated to reflux with an oil bath, and then 4.2 mL of 1-bromopentane was added dropwise into the mixed solution. After refluxing for 24 h, the resulting mixture containing the precipitate KBr was filtered off using a Buchner funnel after a transitory cooling. Subsequently the filtrate was poured into a large amount of water, the white solid precipitate was filtered off and washed with 5% dilute hydrochloric acid and then with distilled water, then dried in an oven to yield crude compound **a**. The purified compound **a** (mp: 147–149 °C, yield: 41%) was obtained by recrystallization from ethanol.

FT-IR (KBr, pellet), cm⁻¹: 3416 (O–H); 2938 (C–H); 1607, 1501 (aromatics); 1248, 1177 (C–O–C). ¹H NMR (CDCl₃), ppm: 7.43–6.84 (m, 6H, Ar–H of naphthalene); 5.18 (s, 1H, hydroxy); 4.00 (m, 2H, –CH₂–O–); 1.38–1.81 (m, 8H, –(CH₂)₄–); 0.95 (t, 3H, methyl).

2.3.2 Synthesis of 6-(hexyloxy)naphthalen-2-yl 3,5-dinitrobenzoate (b). THF (20 mL), triethylamine (1.6 mL) and 6-hexyloxy-2-hydronaphthalen (4.48 g, 0.02 mol) were added to a 100 mL flask placed in an ice bath. After the mixture was

cooled down to 0 °C, a solution of 3,5-dinitrobenzoyl chloride (7.89 g, 0.03 mol) in THF (15 mL) was added dropwise, so that the mixture was maintained between 0 and 5 °C. After the addition was completed, the solution was stirred for 12 h at room temperature and then filtered. The filtrate was added slowly to a vigorously stirred solution of sodium carbonate (32 g) in water (400 mL). The solid was collected by filtration and washed with distilled water three times. The product was recrystallized from a mixed solvent of ethanol and water (7 : 3, v/v) to afford 7.45 g (83%) yellow needle-like crystals: mp 164–166 °C.

FT-IR (KBr, pellet), cm^{-1} : 1749, 1735 (C=O); 2937 (C–H); 1542, 1340 (NO₂); 1609, 1501 (aromatics); 1263, 1138 (C–O–C). ¹H NMR (CDCl₃), ppm: 9.37–9.33 (m, 3H, NO₂–ArH); 7.55–6.93 (m, 6H, Ar–H of naphthalene); 4.01 (m, 2H, –CH₂–O–); 1.39–1.81 (m, 8H, –(CH₂)₄–); 0.95 (t, 3H, methyl).

2.3.3 Synthesis of 6-hexyloxy-naphthalen-3',5'-diaminobenzoate (N6). Reduced iron powder (4.46 g, 0.08 mol), NH₄Cl (2.14 g, 0.04 mol) and a mixed solvent of ethanol and water (3 : 1, v/v, 200 mL in total) was added to a 500 mL flask equipped with a magnetic stirrer and a condenser. After the reaction the mixture was stirred for 1 h at 80 °C and 6-(hexyloxy)naphthalen-2-yl 3,5-dinitrobenzoate (4.38 g, 0.01 mol) was added. The reaction mixture was refluxing in an oil bath for another hour and was monitored by thin layer chromatography (TLC). After the reaction was completed, the hot solution was filtered to remove the impurities and poured into distilled water under vigorous stirring. The crude diamines precipitated as a clear pale yellow solid, which was filtered, thoroughly washed with water, and recrystallized from ethanol; consequently the pure light-yellow solid was obtained. Yield: 78.6%, mp: 152–154 °C.

FT-IR (KBr, pellet), cm^{-1} : 3439, 3366 (NH₂); 2921 (C–H); 1725 (C=O); 1608, 1498 (aromatics); 1227, 1202 (C–O–C). ¹H NMR (CDCl₃), ppm: 7.13–6.95 (m, 6H, Ar–H of naphthalene); 5.97–6.72 (s, 3H, NH₂–ArH); 4.00 (m, 2H, –CH₂–O–); 3.65 (s, 4H, 2–NH₂); 1.39–1.81 (m, 8H, –(CH₂)₄–); 0.97 (t, 3H, methyl).

2.4 Synthesis of the polymers

The PIs were synthesized from various functional diamines (N6 and C6), dianhydride ODPA and assistant diamine DMMDA *via* a two-step method. The molar ratios of N6 and DMMDA were controlled to be 0 : 10 (PI₀–N6), 2 : 8 (PI₂–N6), 3 : 7 (PI₃–N6), 5 : 5 (PI₅–N6), 7 : 3 (PI₇–N6) and 10 : 0 (PI₁₀–N6) to obtain the PI–N6s. The molar ratios of 4-hexyloxy-biphenyl-3',5'-diaminobenzoate (C6) and DMMDA were controlled to be 2 : 8 (PI₂–C6), 3 : 7 (PI₃–C6) and 5 : 5 (PI₅–C6) to attain the PI–C6s.

The synthesis of PI₅–N6 is used as an example to illustrate the general synthetic route to produce the PIs. 5.0 mmol of DMMDA was dissolved in 15 mL of NMP in a 100 mL three-necked flask with mechanical stirring and 10 mmol of ODPA was added to the solution. After a clear solution was formed, 5.0 mmol of N6 was added, and the mixture was stirred at room temperature under a gentle flow of dry nitrogen for 24 h to yield viscous poly(amic acid) (PAA) solutions. PAA was converted into a PI *via* thermal or chemical imidization methods. For the thermal imidization method, PAA solution was cast onto a clean glass plate and heated (80 °C for 30 min,

120 °C for 30 min, 200 °C for 1 h and 250 °C for 2 h) to produce a fully imidized PI film. The chemical imidization method was carried out by the addition of acetic anhydride and pyridine (diamine : acetic anhydride : pyridine = 4 : 36 : 9, molar ratio) to the aforementioned PAA solution (with magnetic stirring) at the ambient temperature for 30 min and *via* heating at 80 °C for 16 h. The PI solution was poured into methanol. The precipitate was collected by filtration, washed thoroughly with hot methanol and dried at 80 °C in a vacuum oven to give PI. Yields were virtually quantitative in every case.

2.5 Fabrication of the liquid crystal cells

PAA solutions diluted to a solid content of 5% in NMP were spin-coated on the clean ITO-coated glass or CaF₂ glass at a speed of 600 rpm for 15 s and 2500 rpm for 30 s followed by heating at 80 °C for 30 min to evaporate the solvent. The films thus obtained spin-coated on glass substrates were cured at 250 °C for 2 h to complete thermal imidization. The prepared PI films on glass were subsequently rubbed with a roller covered commercial rubbing cloth, and the rubbing strength (RS) was calculated as follows:

$$RS = NM(2\pi rn/60v - 1)$$

where RS (mm) was the total length of rubbing cloth that touched a certain point of the films; *N* was the cumulative number of rubbings; *M* (0.3 mm) was the contact length of the rubbing roller circumference; *v* (17.2 mm s⁻¹) was the velocity of the substrate stage. *n* (700 rpm) and *r* (22.5 mm) were the rubbing roller speed and radius, respectively.

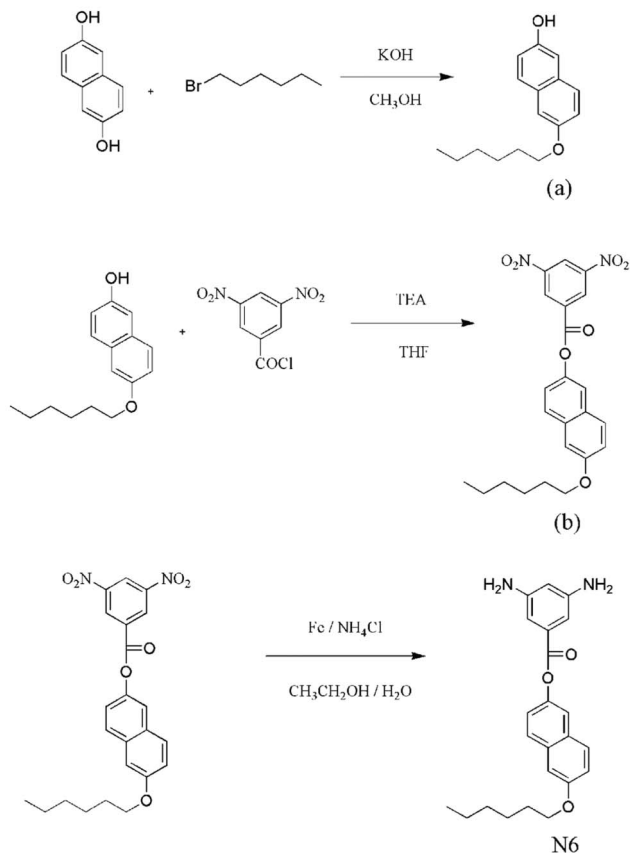
The LC cells were assembled from two pieces of rubbed substrates in an anti-parallel rubbing direction with 20 μm thick spacers. In addition, some non-rubbed substrates were used to fabricate LC cells for comparison. LC E7 was injected into the cell gap using a capillary method at 80 °C, followed by sealing of the injection hole with photo-sensitive epoxy glue. In this study, LC cells were pre-heated to 80 °C before injection to eliminate flow marks in the LC cells. The pretilt angles of LCs were measured using a crystal rotation method.

3. Results and discussion

3.1 Monomer synthesis

The diamine 4-hexyloxy-biphenyl-3',5'-diaminobenzoate (C6) used for comparison was synthesized according to our previous work.²⁵ The novel functional diamine N6 was synthesized from naphthalene-2,6-diol through a three-step synthetic route according to Scheme 1.

First, 6-hexyloxy-2-hydronaphthalen was prepared by the addition of the corresponding 1-bromopentane and potassium hydroxide to a solution of the naphthalene-2,6-diol in methanol; the isolation procedure was carried out using the distinct solubility of the 6-hexyloxy-2-hydronaphthalen and the chief byproduct 6-hexyloxy-2-hexyloxynaphthalen in the alkaline water solution. Subsequently, all 6-hexyloxy-naphthalen-3',5'-dinitrobenzoates were obtained by esterification of 6-hexyloxy-2-hydronaphthalen and 3,5-dinitrobenzoyl chloride



Scheme 1 The synthetic route of the functional diamine **N6**.

in the presence of TEA acting as a catalyst, and the products could be purified by recrystallization.

The final step to obtain the ultimate diamine was the reduction of the corresponding nitrocompound using a neutral reducing agent ($\text{Fe}/\text{NH}_4\text{Cl}$), allowing the synthesis of the diamine in a quantitative yield and pure enough for polycondensation. The oxygen anion is quite stable under the strong conjugate effect from a naphthalene unit, leading to the easy reduction of the ester bond in alkaline or acidic conditions, so a neutral reducing agent was applied to the final step instead of the common reduction systems, such as Pd/C in hydrazine hydrate (a strongly alkaline reducing agent) and SnCl_2 in hydrochloric acid (a strongly acidic reducing agent).

The chemical structures of all above compounds were confirmed by melting point analysis, FT-IR and ^1H NMR spectra. All the spectroscopic data obtained were consistent with the proposed structures. The ^1H NMR spectrum of the functional diamine is displayed in Fig. 1.

3.2 Polymer synthesis

New PIs were prepared from **N6** or **C6**, assistant diamine DMMDA and commercially available aromatic dianhydride (ODPA) *via* a conventional two-step procedure as shown in Scheme 2. The polymerization was carried out by reacting stoichiometric amounts of the diamines with aromatic dianhydrides at a concentration of 15% solids in NMP. The

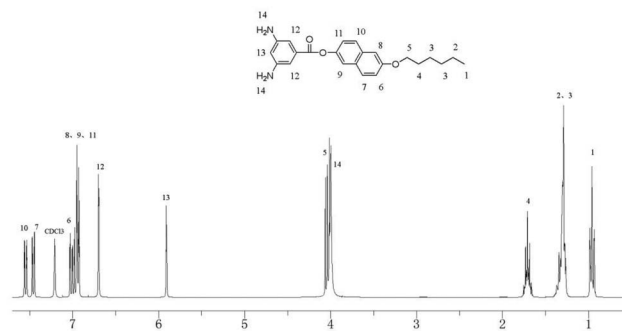
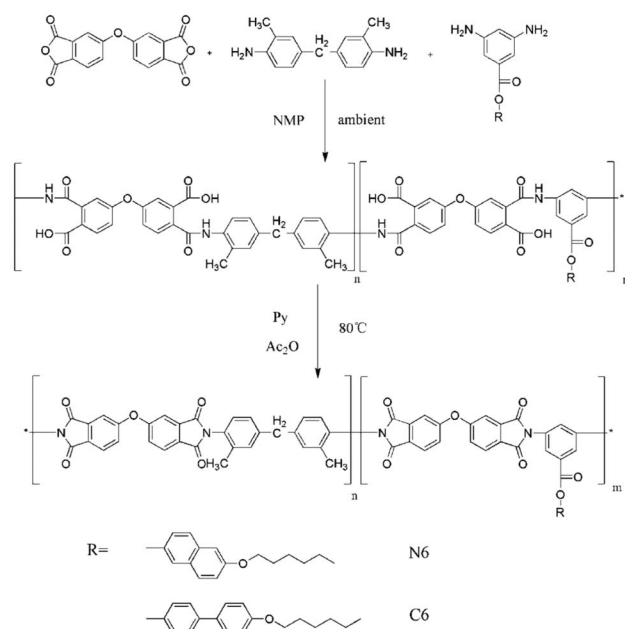


Fig. 1 The ^1H NMR spectra of the functional diamine **N6**.

ring-opening polymerization at room temperature for 24 h yielded PAAs, followed by sequential heating to $250\text{ }^\circ\text{C}$ or the addition of a mixture of Ac_2O and Py to obtain the corresponding polymers. Transformation from PAA to PI was possible *via* the thermal or chemical cyclodehydration; the merits of the former were the product was easy to handle and to cast into thin films, and the latter was suited to prepare soluble PIs. The chemical imidization method allowed high yields and high-molecular-weight PIs to be achieved in every case. The yields and molecular weight of the isolated PIs have been summarized in Table 1.

All of the polymers were characterized by spectroscopic techniques, in particular IR and NMR spectroscopy. As an example, the ^1H NMR spectrum of one polymer is shown in Fig. 2, where all the signals could be readily ascribed to the protons of the polymer. IR spectra of the various polymers showed absorption bands typical of aliphatic C–H stretching at $2927\text{--}2863\text{ cm}^{-1}$, corresponding to the methyl groups of the diamine **N6**. Strong bands at 1778 and 1724 cm^{-1} due to the



Scheme 2 The synthetic route for the polymers.

Table 1 Intrinsic viscosity, molecular weight and elemental analysis of PIs

Sample	η_{inh}^a (dL g ⁻¹)	Yields ^a (%)	M_n^a ($\times 10^{-4}$ g Mol ⁻¹)	M_w/M_n	Elemental analysis ^b			
					C (%)	H (%)	N (%)	
PI ₀ ^c	1.12	95	1.81	1.91	Calc.	74.40	4.00	5.60
					Found	73.91	3.89	5.81
PI ₂ -N6	0.34	90	1.55	1.67	Calc.	71.84	3.83	6.71
					Found	70.55	3.71	6.89
PI ₃ -N6	0.25	87	1.36	1.89	Calc.	71.66	3.90	6.43
					Found	70.01	3.77	6.52
PI ₅ -N6	0.23	85	1.09	1.83	Calc.	71.34	4.03	5.94
					Found	69.86	3.91	6.41
PI ₇ -N6	—	82	0.89	1.85	Calc.	71.06	4.15	5.53
					Found	69.39	4.02	6.26
PI ₁₀ -N6	—	81	0.63	1.77	Calc.	70.71	4.29	5.00
					Found	68.88	4.06	5.84

^a Measured at a polymer concentration of 0.5 g dL⁻¹ in NMP at 30 °C, PIs were obtained by chemical imidization. ^b Samples prepared by thermal imidization. ^c PI₀ was prepared by polymerization of ODPa and DMDA.

symmetrical and unsymmetrical vibrations of the two imide carbonyl groups, were also observed for all polymers, along with a sharp absorption band around 725 cm⁻¹ associated to the skeletal vibration of the imide rings. Absorption bands appearing at 1375 cm⁻¹ and 1244–1103 cm⁻¹ belonged to the vibrations of C–N and C–O–C units, respectively. Spectroscopic data are also in agreement with an essentially complete imidization (Fig. 3).

The data of inherent viscosity and GPC measurements listed in Table 1 indicate high molecular weights in the range of 0.63–1.81 $\times 10^4$ g mol⁻¹ for M_n . The elemental analyses obtained agree quite well with calculated values for the proposed structures of the PIs. This is consistent with the fact that creasable films could be obtained by casting and solvent evaporation of polymer solutions.

3.3 Solubility

The solubility of the PIs was investigated in different solvents (Table 2). Satisfactorily, all polymers could be dissolved in

polar solvents, such as cresols, NMP, or DMAc at room temperature in most cases and even showed outstanding solubility in common organic solvents, like THF, chloroform and so on. The favorable solubility is most likely due to the combination of the steric and polar nature of the carbonyl units of both functional dimines (N6 and C6), which greatly favors solubility in polar organic media. Also, the steric hindrances of the –CH₃ and flexible segments (–CH₂–) twists the rings of the main chains dramatically out of plane, resulting in a noncoplanar and contorted conformation capable of efficiently hindering the chain packing. All factors reduce the chain–chain interaction and enhance solubility.

PI films fabricated by casting from the NMP solutions were characterized using X-ray diffraction (XRD), showing only an amorphous halo and no indication of crystallinity (Fig. 4), which further explains the good solubility observed.

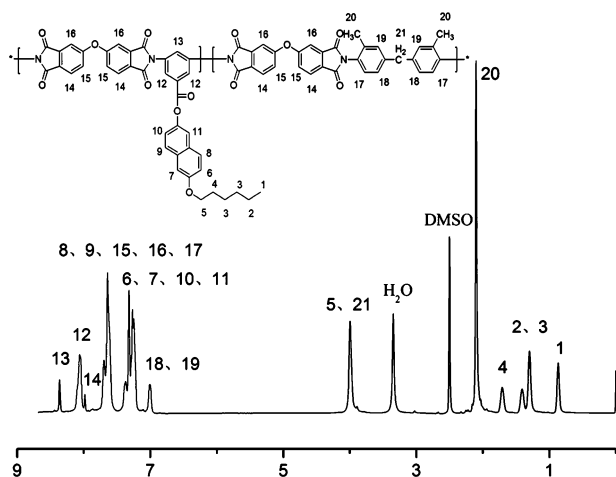
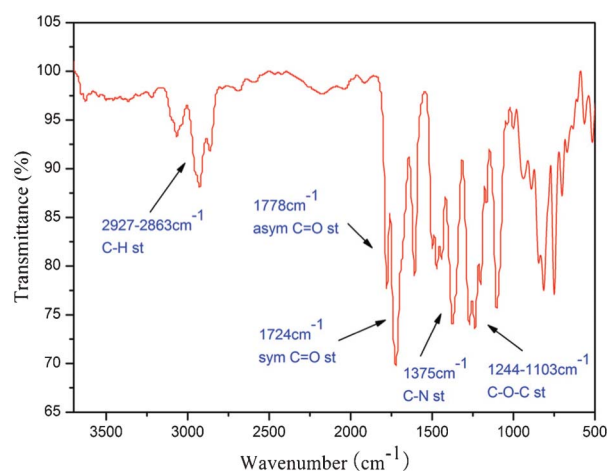
**Fig. 2** The ¹H NMR spectra of a polymer.**Fig. 3** The FT-IR spectra of PI₂-N6.

Table 2 Solubility of the PIs in different solvents

PIs ^a	NMP	DMSO	DMF	DMAc	<i>m</i> -cresol	TCM	THF
PI ₀	+–	+–	+–	+–	+–	++	+
PI ₂ -N6	++	++	++	++	++	++	++
PI ₂ -C6	++	++	++	++	++	++	++
PI ₃ -N6	++	++	++	++	++	++	++
PI ₃ -C6	++	++	++	++	++	++	++

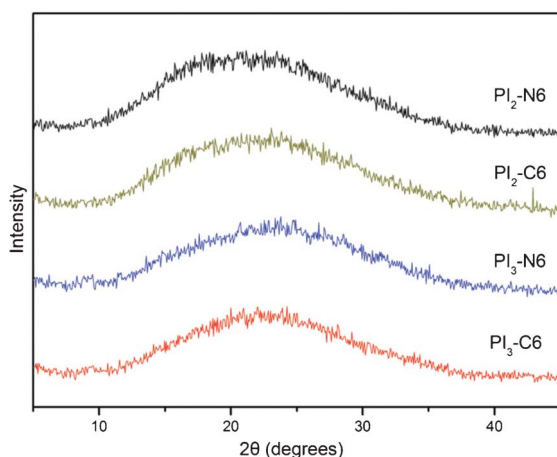
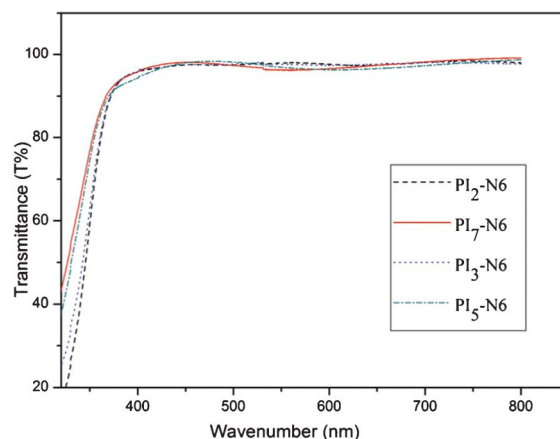
^a Qualitative solubility was determined with 10 mg of the polymer in 1 ml of solvent. (++) soluble at room temperature, (+) soluble upon heating, (+–) partially soluble upon heating.

3.4 Optical transparency

The optical transparency of the novel PI-N6 films was studied using UV-visible spectra. The films obtained by casting from a 5 wt% solution on a calcium fluoride (CaF₂) piece all showed high transmission (>95%) in the wavelength range of 400–700 nm. As shown in Fig. 5, the curves of optical transparency were shifted toward the low wavelength with the an increasing side-chain content. This was attributed to the incorporation of the bulky hexyloxy-naphthalen groups which decreased the charge-transfer complex (CTC) effect between backbones. On the other hand, the introduction of an aliphatic unit (–CH₂–) into the PI backbone would also facilitate less intramolecular CTC interactions, lowering the color of these PIs. The high optical transparency of PI films is advantageous in LCD devices.

3.5 Characterization of the liquid crystal display cells

3.5.1 Pretilt angle. The pretilt angle is an important parameter that determines the optical properties of LCD devices. The pretilt angle can be affected by various factors, such as surface energy, surface morphology, steric effects and the electronic interaction of the LC with the alignment layer, *etc.* This might be caused by a processing condition like the rubbing treatment as well as the chemical structure of the PI. As is well known, the rubbing treatment is a widely used

**Fig. 4** Wide-angle XRD patterns of the polymers.**Fig. 5** The transmittance of PI-N6.

technique to provide the homogeneous alignment of the LC molecules onto the polymer surface. Thus, a lot of research has been carried out in order to understand the physical mechanism responsible for the LC alignment on the polymer surface. In this study, a series of PAAs with molecularly designed structures were synthesized and the effect of the rigid part (naphthalene unit) of N6 on the pretilt angle after the rubbing process was investigated. Furthermore, the relationship between the pretilt angle and the molar fraction of N6 to total diamines used has been studied.

3.5.2 Effect of the content of functional diamine on the pretilt angle. As illustrated in Fig. 6, the pretilt angles of the LC cells fabricated using the novel PIs before the rubbing treatment ranged from 89 to 90° except for PI₀. The pretilt angle of PI₀ was not detected before the rubbing treatment because the LC was not aligned on the surface of the PI₀ film. However, the pretilt angles of the LC cells fabricated with PI₂₋₁₀-N6 containing N6 equal to or greater than 20 mol% to the total amount of the diamines used ranged from 89 to 90°

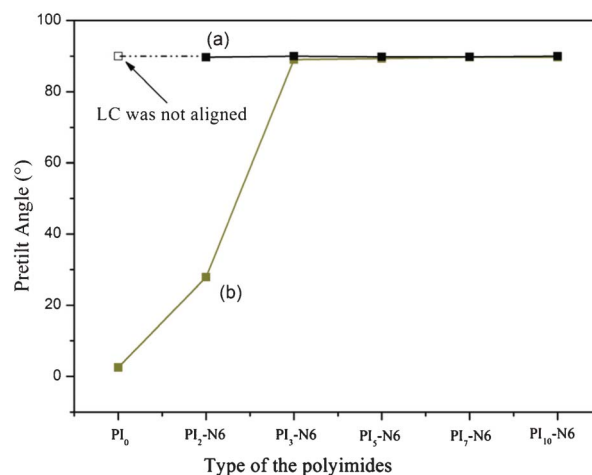
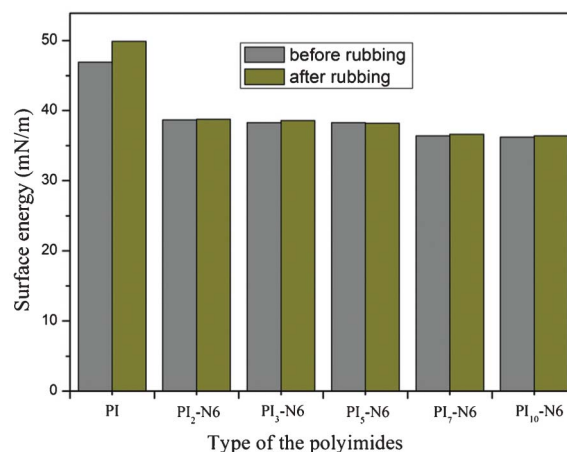
**Fig. 6** Pretilt angles of the LC cells fabricated with the PIs as LC alignment layers (a) before and (b) after the rubbing treatment (rubbing strength was 56.9 mm).

Table 3 Variation of the surface energy of the polyimides before and after the rubbing treatment

Polyimide	Contact angle (°)		Surface energy (dyn cm ⁻¹)
	Water	Diiodomethane	
Before the rubbing treatment			
PI ₀	70.8	30.1	46.9
PI ₂ -N6	78.1	46.0	38.7
PI ₃ -N6	78.3	46.7	38.3
PI ₅ -N6	78.8	46.2	38.3
PI ₇ -N6	78.7	50.8	36.4
PI ₁₀ -N6	79.1	50.8	36.2
After the rubbing treatment			
PI ₀	68.6	22.1	49.9
PI ₂ -N6	77.6	46.0	38.8
PI ₃ -N6	77.6	46.7	38.6
PI ₅ -N6	77.7	47.3	38.2
PI ₇ -N6	78.3	48.0	36.6
PI ₁₀ -N6	79.0	50.1	36.4

before the rubbing treatment. This was due to the very low surface energies of the PI₂₋₁₀-N6 ranging from 36.2 to 38.7 dyn cm⁻¹. Table 3 shows the contact angles of water and diiodomethane on the PI films, from which the surface energies were calculated by the harmonic mean equation before and after the rubbing treatment. As shown in Table 3, with an increase in the content of the hexyloxy-naphthalen groups, the water contact angles on the PIs were increased both before and after rubbing, which was due to a decrease in the surface polarity of the PI films with the introduction of the hexyloxy-naphthalen groups. In particular, the surface energy of the PI was remarkably decreased from 46.9 to 38.7 dyn cm⁻¹ with the introduction of 20 mol% of N6. Furthermore, the surface energy slightly decreased to 36.2 dyn cm⁻¹ with an increased content of naphthalene side chains, which resulted in high pretilt angles above 89°. This revealed similar results to our previous studies, which showed that the pretilt angle increased with a decrease in the surface energy of the PI films or an enrichment of the long alkyl side chains on the PI surface.²³

3.5.3 Effect of rubbing treatment on the pretilt angle. The surface of PIs is the core of research into the alignment layers since it straightforwardly contacts, aligns LC molecules and generates pretilt angles for LC molecules. The surface energies can supply some information about the surface. As shown in Fig. 7, the surface energies of the PI films were compared before and after the rubbing treatment. As summarized in Table 3, they were slightly increased by the rubbing treatment, which resulted in an increase in the surface polarity of the PI film and a decrease of the pretilt angles. That is, the rubbing process induced the increase in the polarity of the PI films by an insertion of the naphthalen side group of the N6 into the polymer bulk phase during the rubbing process. This resulted in an increase in the polarity of the PIs containing long alkyl side chains and the increase in the flatness of the thin film to make the LC molecules lie flatter. However, the surfaces of the PI₂₋₁₀-N6 films were saturated by the naphthalen side group above a composition of 20 mol% of N6, which resulted in a

**Fig. 7** Variation in the surface energy of the polyimides films.

very high pretilt angle above 89° even after the rubbing process. The novel PI with a long alkyl chain was connected with a particularly rigid naphthalene unit. That is, the rigid naphthalene connecting group may restrict the movement of the long alkyl chain into the polymer surface, which results in the low surface energy and an enrichment of non-polar alkyl side chains at the outmost layer of the PI surface. As a result, the PI obtained from N6 with a rigid naphthalene group showed a high pretilt angle above 89° even after rubbing treatment.

Conoscope observations of the LC cells were obtained with a polarized optical microscope. As shown in Fig. 8, the dark crossed brush was seen clearly and did not move with the LC cell rotating before and after rubbing. The result further proved the vertical alignment was induced by PI with naphthalene side chains.

3.6 Thermal properties and the mechanism of imidization

DSC and TGA methods were applied to evaluate the thermal properties of the PIs, and thermal analysis data from the TGA and DSC curves of the PIs are summarized in Table 4. DSC revealed that rapid cooling from 300 °C to room temperature produced predominantly amorphous samples. The T_g values of

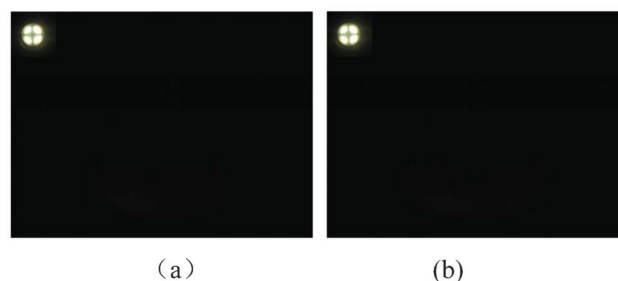
**Fig. 8** Polarized optical microscopic image of vertical LC. All of the pictures were captured under crossed polarizers. The conoscopic images are shown in the corner of the picture. (a) Before rubbing, (b) after rubbing. The alignment film is PI₃-N6.

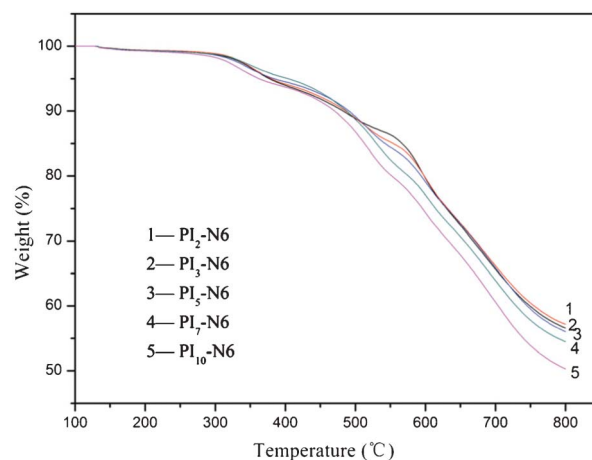
Table 4 The thermal properties of the PIs

PIs ^a	T_g^b (°C)	T_d^c (°C)	T_5^c (°C)	T_{10}^c (°C)	R_w^c (%)
PI ₂ -N6	244	373	443	470	57.9
PI ₂ -C6	243	371	435	466	56.9
PI ₃ -N6	235	354	438	451	56.6
PI ₃ -C6	232	355	421	446	54.8
PI ₅ -N6	230	338	416	437	49.5
PI ₅ -C6	221	333	409	430	48.1

^a Measured samples were obtained by the thermal imidization method. ^b T_g , the glass-transition temperature, was measured using DSC at a heating rate of 10 °C min⁻¹ in air. ^c T_d , decomposition-starting temperature; T_5 and T_{10} , temperature at a 5 or 10% weight loss; R_w , residual weight (%) at 800 °C in nitrogen.

PI-N6 were in the range of 221–244 °C. As we expected, the T_g values of these PIs depended on the structure of the different components and decreased with increasing flexibility of the PI backbones according to the applied structure of the monomer. Compared with the PIs from C6, PIs from N6 show a slightly higher T_g . N6 is shorter than C6 when they possess the same length of alkyl chain, so N6 brought about smaller steric configuration, resulting in tighter chain packing of PI-N6. The segments of the chain could only move under higher temperatures, so higher T_g s were observed for PI-N6.

In order to investigate the thermal stability of the PIs, the thermal imidization method was adopted to produce PIs rather than chemical imidization method, because soluble PIs from the chemical imidization method are usually linear polymers which tend to absorb water which may exert unexpected influence on the results. The difference in the PIs produced by thermal and chemical imidization could be explained by the imidization reaction mechanism as discussed later in this section. Table 4 gives the temperatures of the initial decomposition (T_d) and 5% (T_5) and 10% (T_{10}) gravimetric losses in nitrogen. From Table 4, we can see PI-N6 exhibited slightly higher T_d and T_{10} , but much higher T_5 compared with the corresponding PI-C6. Research has shown that PIs containing side chains exhibit distinct two-step weight loss behaviors.²⁹ The weight loss percentage during the first degradation was equivalent to the weight fraction of the side chain, indicating that the values of T_d and T_5 had a close relationship with the structure of side chains. Both functional diamines possessed the same long alkyl chains and the backbone of PIs were also the same, so similar values of T_d were observed. The planar naphthalene unit was more rigid than the twisted biphenyl unit, so the introduction of naphthalene groups into N6 increased the rigidity of the side chains of PI-N6, but decreased the weight ratio of the side chains simultaneously. Higher values of T_5 demonstrated that PI-N6 was more thermally-stable than PI-C6. The second degradation corresponded to the thermal degradation of the polymer main chain.²⁹ As they contain the same alkyl chain and are similar in structure, the two kinds of PIs obtained from the two functional diamines had similar structures, so close values of T_{10} and R_w were found. The TGA results show

**Fig. 9** The TGA curves of the PI-N6s.

that the introduction of a naphthalene unit into the side chain could effectively improve the thermal stability of soluble PIs.

The TGA curves of PI-N6 from thermal imidization are displayed in Fig. 9. The favorable thermal stability from the thermal imidization method was possibly due to the presence of partial intermolecular crosslinking, as shown in Fig. 10. The difference between PIs produced by thermal and chemical imidization can be explained by the imidization reaction mechanism. PAA was synthesized by dianhydride and diamine *via* a polyaddition reaction in the amide type polar solvent at room temperature. This kind of PAA was an unstable polymer, a nucleophilic substitution reaction was caused, substituting the hydroxyl group of the carboxylic acid group and amino group of amide in PAA, respectively, with the carbonyl group of PAA. The former (hydroxyl group with the carbonyl group) was a reversible reaction, which could reduce to form anhydride and amine at room temperature or in the heating process, and the latter (amino group with the carbonyl group) was an irreversible reaction, which would dehydrate to form imide only in the heating process. At room or low temperatures, the equilibrium of the former tends to become PAA solution with little chance for a decomposition reaction to occur. However, when PAA solution was heated, the reversible and irreversible reactions increased with temperature, and more anhydride ends and amine ends in PAA were produced. The ketone group of the side chain was an electrophilic group, which condensed to the amine group to form an imine group; therefore, PAA with the ketone group is connected with imine linkage to form nonlinear or crosslinking PI during thermal imidization. The crosslinking reaction increased with a higher concentration of PAA after most solvents were volatilized in the imidization. If PAA is tested with Ac₂O and Py *via* chemical imidization, causing the Ac₂O to react with amic acid to form amide-anhydride, then the imide is formed by a nucleophilic reaction of the amide-anhydride group with separating acetic acid. That is, a crosslinking reaction would not occur in chemical imidization. According to the preceding description, this type of crosslinking was due to the ketone group of PAA being connected with the imine group by thermal imidization.

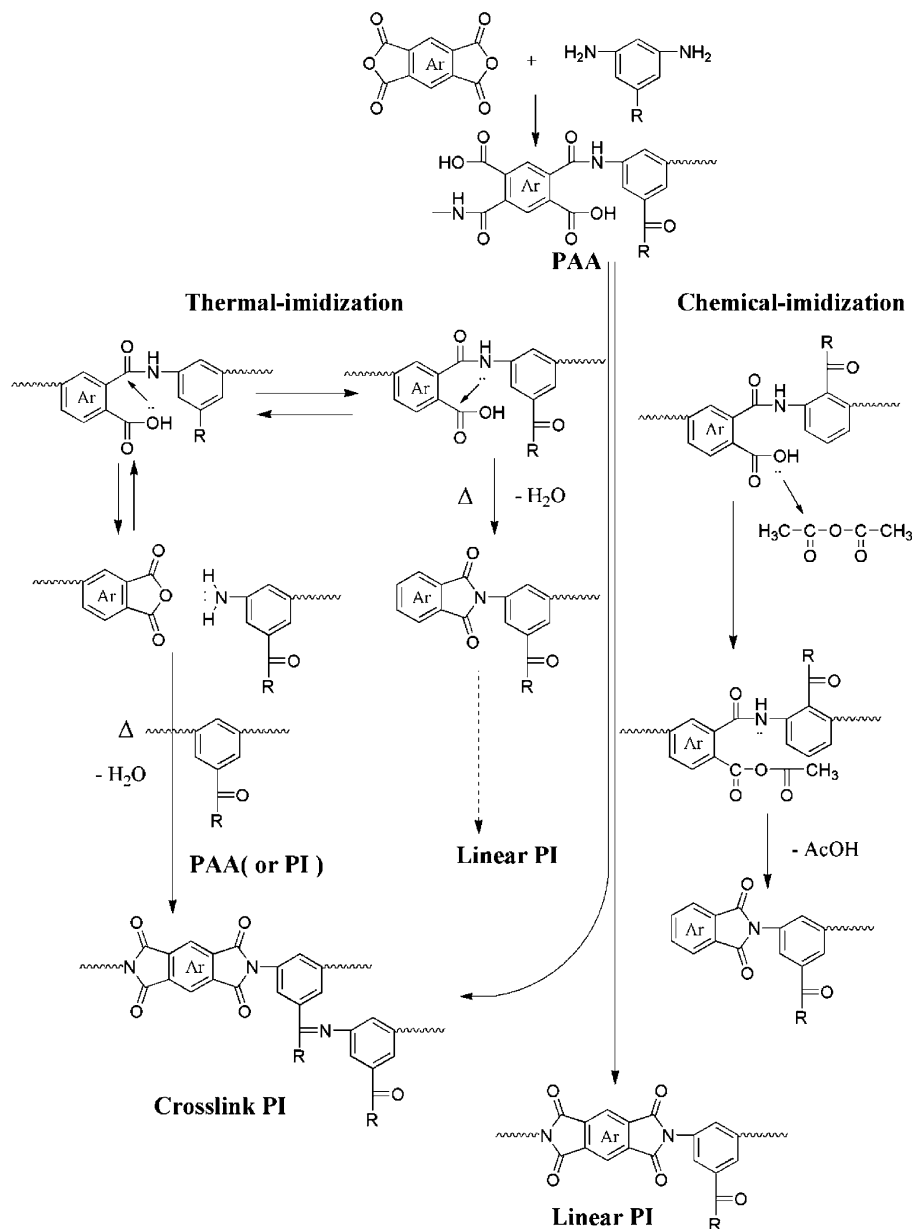


Fig. 10 The mechanism of chemical and thermal imidization.

4. Conclusion

Novel functional diamine (**N6**) containing a rigid naphthalene unit, was molecularly designed and successfully synthesized. PIs were obtained by copolymerization of **N6**, DMMDA and ODPA. The structures of the intermediates, diamines and PIs were confirmed using FT-IR and 1H NMR spectra. All PIs obtained could be dissolved in polar aprotic solvents and low-boiling-point solvents. PI films attained by a casting method showed favorably high transmittance above 95% in the wave length range of 400–700 nm and could align LCs vertically before and after rubbing treatment. PI-**N6** exhibited a slightly higher T_d and T_{10} , but much higher T_5 compared with the corresponding PI-**C6**. For PI-**N6**, the weight ratio of the side

chains was smaller than that of PI-**C6**, but a much higher T_5 was attained. The results demonstrated that the introduction of a naphthalene unit into the side chain could effectively improve the thermal stability of the PI without sacrificing its solubility. In addition, the difference between PIs produced by thermal and chemical imidization was explained in a preliminary manner by the imidization reaction mechanism.

Acknowledgements

This work was supported by National Natural Science Foundation of China (Grant No. 51173115), the Ministry of Education (the Foundation for Ph.D. training, Grant No.

20110181110030) of China and the Scientific Research Foundation for the Returned Overseas Chinese Scholars, State Education Ministry, and Science (No. 20071108-18-12).

Notes and references

- M. Calle, A. E. Lozano, J. G. de la Campa and J. de Abajo, *Macromolecules*, 2010, **43**, 2268.
- C. Garcia, A. E. Lozano, J. G. de la Campa and J. de Abajo, *Macromol. Rapid Commun.*, 2003, **24**, 686.
- Y.-T. Chen and J.-Y. Tsai, *Macromolecules*, 2008, **41**, 9556.
- G. C. Eastmond and J. Paprotny, *Macromolecules*, 1996, **29**, 1382.
- A. Ghosh, S. K. Sen, S. Banerjee and B. Voit, *RSC Adv.*, 2012, **2**, 5900.
- G. C. Eastmond, M. Gibas and J. Paprotny, *Eur. Polym. J.*, 1999, **35**, 2097.
- L. J. Mathias, A. V. G. Muir and V. R. Reichert, *Macromolecules*, 1991, **24**, 5232.
- T. Matsuura, Y. Hasuda, S. Nishi and N. Yamada, *Macromolecules*, 1991, **24**, 5001.
- F. Li, J. J. Ge, P. S. Honigfort, S. Fang, J.-C. Chen, F. W. Harris and S. Z. D. Cheng, *Polymer*, 1999, **40**, 4987.
- F. Li, S. Fang, J. J. Ge, P. S. Honigfort, J.-C. Chen, F. W. Harris and S. Z. D. Cheng, *Polymer*, 1999, **40**, 4571.
- S.-H. Hsiao, C.-P. Yang and C.-Y. Yang, *J. Polym. Sci., Part A: Polym. Chem.*, 1997, **35**, 1487.
- D. S. Reddy, C.-F. Shu and F.-l. Wu, *J. Polym. Sci., Part A: Polym. Chem.*, 2002, **40**, 262.
- T. Matsumoto and T. Kurosaki, *Macromolecules*, 1997, **30**, 993.
- T. Matsuura, M. Ishizawa, Y. Hasuda and S. Nishi, *Macromolecules*, 1992, **25**, 3540.
- T. Matsuura, N. Yamada, S. Nishi and Y. Hasuda, *Macromolecules*, 1993, **26**, 419.
- T. Matsuura, S. Ando, S. Sasaki and F. Yamamoto, *Macromolecules*, 1994, **27**, 6665.
- K.-W. Lee, S.-H. Paek, A. Lien, C. Durning and H. Fukuro, *Macromolecules*, 1996, **29**, 8894.
- H. W. David, Z. Shen, M. Guo, S. Z. D. Cheng and F. W. Harris, *Macromolecules*, 2007, **40**, 889.
- C. Cai, A. Lien, P. S. Andry, P. Chaudhari, R. A. John, E. A. Galligan, J. A. Lacey, H. Ifill, W. S. Graham and R. D. Allen, *Jpn. J. Appl. Phys.*, 2001, **40**, 6913.
- S. K. Sen and S. Banerjee, *RSC Adv.*, 2012, **2**, 6274.
- B. S. Ban, Y. N. Rim and Y. B. Kim, *Liq. Cryst.*, 2000, **27**, 125.
- C.-J. Guo, Z. Sun, S.-L. Xia and Y.-H. Wang, *Liq. Cryst.*, 2012, **39**, 721.
- J. Wang, L. Wang, Y. Zeng, Y.-Q. Fang, Q. Zhang and Y. Wang, *Liq. Cryst.*, 2010, **37**, 271.
- H. Awano, Y. Kanno, T. Takahashi, K. Yonetake, S. Ishida, Y. Kawasumi and A. Hirai, *Liq. Cryst.*, 2011, **38**, 1137.
- Z. Liu, F. Yu, Q. Zhang, Y. Zeng and Y. Wang, *Eur. Polym. J.*, 2008, **44**, 2718.
- Y.-Q. Fang, J. Wang, Q. Zhang, Y. Zeng and Y.-H. Wang, *Eur. Polym. J.*, 2010, **46**, 1163.
- T. Sakai, K. Ishikawa and H. Takezoe, *Liq. Cryst.*, 2002, **29**, 47.
- J. M. Geary, J. W. Goodby, A. R. Kmetz and J. S. Patel, *J. Appl. Phys.*, 1987, **62**, 4100.
- S. I. Kim, M. Ree, T. J. Shin and J. C. Jung, *J. Polym. Sci., Part A: Polym. Chem.*, 1999, **37**, 2909.